Matr3 reshapes m6A modification complex to alleviate macrophage inflammation during atherosclerosis

Zewei Sun
Zhejiang University
Wenjing Chen
Zhejiang University
Zhen Wang
Zhejiang University
Shuai Wang
Hangzhou First People's Hospital
Jie Zan
Guangdong University of Technology
Wenting Zhao (11518182@zju.edu.cn)
Zhejiang University https://orcid.org/0000-0002-4742-6223

Research

Keywords: Atherosclerosis, N6-methyladenosine (m6A) modification, Mettl14, Matrin-3, Macrophage

Posted Date: June 16th, 2022

DOI: https://doi.org/10.21203/rs.3.rs-1710402/v1

Abstract

Background

Atherosclerosis, characterized as the chronic inflammation of the arterial wall, is one of the leading causes of coronary artery disease (CAD), and macrophages are found to play essential roles in the initiation and progression of inflammation in atherosclerosis. N6-methyladenosine (m6A) modification, as the most abundant epi-transcriptomic modification in mRNA, is found to mediate the atherogenic inflammatory cascades in vascular endothelium. The detailed molecular mechanism of m^6A methylation regulating inflammatory response during atherosclerosis is still not fully known.

Results

In this study, we find oxidized low-density lipoprotein (oxLDL) stimulation increases methyltransferases Mettl3 and Mettl14 expressions in macrophages, whereas the total m6A modification level in macrophages decreases under oxLDL stimulation. Matrin-3 (Matr3), an RNA binding protein, is identified to function a suppressive role on oxLDL-mediated macrophage inflammatory responses through inhibiting activation of pro-inflammatory signaling, mitogen-activated protein kinase (MAPK) by m6A-mediated mRNA decay via regulating the formation of Mettl3-Mettl14 complex. Moreover, we find that Matr3 expression decreases in the oxLDL-stimulated macrophages, and the peripheral blood mononuclear cells from patients with CAD, and overexpression of Matr3 significantly alleviates atherosclerosis development *in vivo*.

Conclusion

Our study for the first time clarifies the role of Matr3 on macrophage inflammatory responses during atherosclerotic development, and supplies deep understanding on the relationship of m6A modification and inflammatory responses in atherosclerosis.

Introduction

Atherosclerosis, characterized as the chronic inflammation of the arterial wall, is the major cause of coronary artery disease (CAD) which is the leading cause of death in the world[1]. Formation of atherosclerotic plaque is the characterized pathology of atherosclerosis[2]. Nowadays, macrophages have been proved to play essential roles in initiation and progression of inflammation in atherosclerosis, and are closely associated with the formation of atherosclerotic plaque[3, 4]. Initially, elevated modified low density lipoprotein (LDL) in the serum, such as oxidized low-density lipoprotein (oxLDL), is cytotoxic and leads to vascular endothelial injury[5, 6]. Then, monocytes in the blood are attracted by adhesion molecules from injured endothelial cells to emigrate into the injured arterial intima, where monocytes differentiate to macrophages to produce pro-inflammatory factors and phagocytize oxLDL and

cholesterol, gradually resulting in formation of foam cell formation and necrotic core of atherosclerotic plaques[7, 8]. Besides drugs which lower cholesterol are widely used to treat atherosclerosis, recent studies have reported that inhibiting the inflammatory component of atherosclerosis could also effectively decrease atherosclerosis[9, 10].

Up to now, many risk factors are reported to contribute to atherosclerosis, including smoking, hypercholesterolemia, hypertension, hyperglycemia, genetic factors, and epigenetic factors[11–14]. The N6-methyladenosine (m6A) modification is the most abundant epi-transcriptomic modification in mRNA, and plays important roles in various diseases, such as obesity, cancers, hypertension and viral infection through regulating RNA stability, export, splicing or translation[15, 16]. mRNA m6a modification is mainly catalyzed by the methyltransferase-like 3 (Mettl3)/METTL14 heterodimer, and demethylated by de-methyltransferases, such as fat-mass and obesity-associated protein (FTO) and α-ketoglutarate-dependent dioxygenase alkB homolog 5 (ALKBH5)[17, 18]. m^6A methylated mRNA is then directly recognized by “reader” proteins, such as YTH (YT521-B homology) domain family (YTHDF) proteins and insulin-like growth factor 2 (IGF2) mRNA binding proteins (IGF2BP) to affect mRNA decay or translation[19, 20]. Recent study reports a marked downregulation of m6A in rRNA through analyzing carotid atherosclerotic lesion samples representing early and advanced stages of atherosclerosis compared to non-atherosclerotic arteries from healthy controls[21]. Furthermore, Mettl3-dependent m6A RNA modification is reported to mediate the atherogenic inflammatory cascades in vascular endothelium[22]. However, the detailed molecular mechanism of m^6A methylation regulating inflammatory response during atherosclerosis is still not fully known.

In this study, we find oxLDL stimulation increases methyltransferases Mettl3 and Mettl14 expressions in macrophages, whereas the total m6A modification level in macrophages decreases under oxLDL stimulation. Matrin-3 (Matr3), an RNA binding protein, is identified to function a suppressive role on oxLDL-mediated macrophage inflammatory responses through inhibiting activation of pro-inflammatory signaling, mitogen-activated protein kinase (MAPK) by m6A-mediated mRNA decay via regulating the formation of Mettl3-Mettl14 complex in macrophages. Moreover, we find that Matr3 expression is decreased in the oxLDL-stimulated macrophages, and the peripheral blood mononuclear cells from patients with CAD, and overexpression of Matr3 significantly alleviates atherosclerosis development *in vivo*. Our study for the first time clarifies the role of Matr3 on macrophage inflammatory responses during atherosclerotic development, and supplies deep understanding on the relationship of m6A modification and inflammatory responses in atherosclerosis.

Methods And Materials

Ethics statement

Approval for this study was issued by the Ethics Committee of the First Affiliated Hospital, College of Medicine, Zhejiang University, China. Patients gave informed consent upon hospitalization.

Human PBMC isolation

The peripheral blood samples from patients with coronary artery disease and healthy volunteers were obtained from the First Affiliated Hospital, College of Medicine, Zhejiang University. Peripheral blood mononuclear cells (PBMCs) were isolated using PBMC isolation kit (Solarbio, China). Informed consent was obtained from all participants in accordance with the guidelines of the Human Subjects Committee of the Medical Ethical Commission of the First Affiliated Hospital of Zhejiang University (China) and the declaration of Helsinki.

Cell culture

Human THP-1 monocytes and human embryonic kidney cells (HEK-293T) cells were cultured with DMEM supplemented with 10% FBS (Gibco, USA). To facilitate differentiation into macrophages, THP-1 monocytes were treated with 100 nM PMA for 24 h. Subsequently, the macrophages were washed using serum free medium and then prepared for the following experiment.

RNA extraction and real-time PCR analysis

Total RNA was extracted using an RNA prep Pure Cell/Bacteria Kit (Tiangen, China), and then reverse-transcribed into cDNA using PrimeScript RT Master Mix (Takara, Japan). SYBR Premix Ex TaqII (Takara, Japan) kit was used for RT-PCR detection with ABI PRISM 7500 Detection System (ABI, USA). Values were normalized by GAPDH. The primers used were as follows: GAPDH, 5'-GGAGCGAGATCCCTCCAAAAT-3' and 5'-GGCTGTTGTCATACTTCTCATGG-3'; MAP3K11, 5'-GCAGCCCATTGAGAGTGAC-3' and 5'-CACTGCCCTTAGAGAAGGTGG -3'; MAPK14, 5'-CCCGAGCGTTACCAGAACC-3' and 5'-TCGCATGAATGATGGACTGAAAT-3'; PGC-1α, 5'-TCTGAGTCTGTATGGAGTGACAT-3' and 5'-CCAAGTCGTTCACATCTAGTTCA-3'; Matr3, 5'-ATCAATGGAGCAAGTCACAGTC-3' and 5'-TGCAACATGAATGGATCACCC-3'

All samples were quantitated using the comparative CT method and normalized to GAPDH.

Dot blot

Macrophages were treated with oxLDL (+, 40 μg/ml; ++, 80 μg/ml) or not for 24 h. Then, the cells were collected and total RNA was extracted, and spotted on the Immobilon-NC Transfer Membrane (Merck) and UV crosslinked to the membrane. After washing by 1 × TBS with 0.1% Tween-20 buffer (TBST), the membrane was blocked in 1 × TBST with 5% non-fat milk for 1 h and incubated with primary m6A antibodies (1:1000, ab284130, Abcam) overnight at 4 °C. After incubating with goat anti-rabbit IgG antibody conjugated to horseradish peroxidase, the membrane was developed using the ECL kit (Pierce, USA).

Plasmids, siRNAs, and cellular transfection

pCMV3-N-FLAG-Mettl3 plasmid (HG23100-NF) and pCMV3-N-FLAG-Mettl14 plasmid (HG26794-NF) were purchased from SinoBiological (Beijing, China). pCMV3-N-Myc-Matr3 and pEGFP-C3-Matr3 plasmids were synthesized by Sangon (Shanghai, China). small interfering RNAs (siRNAs) against Mettl3 (si-Mettl3) and scrambled siRNA (si-NC) were synthetized by GenePharma (Shanghai, China). The cellular transfections were performed as follows: Cells were cultured in serum-free medium for 30 min before transfection. A total of 2 μl of siRNA or plasmid and 3.3 μl of RNAiMAX reagent (Invitrogen, USA) were mixed, incubated for 10 min, and added to each well. Culture medium was changed with FBS containing culture medium six hours later. The plates were allowed to incubate at 37 °C for 24 h for subsequent detection.

Western blotting

Macrophages were treated with oxLDL of different concentrations for 24 h. Cells were lysed using cell lysis buffer (CST, USA) to extract the total protein, which were then detected using the BCA protein assay kit (Thermo, USA). Protein samples were separated on a 10% SDS-PAGE gel and then transferred to PVDF membranes (Millipore, USA). The membranes were blocked with 5% non-fat milk for 1 h at room temperature and then incubated overnight at 4 °C with the following primary antibodies: rabbit anti-GAPDH (1:1000, Sangon, China), rabbit anti-Mettl3 (1:1000, ab195352, Abcam), rabbit anti-Mettl14 (1:1000, ab252562, Abcam), rabbit anti-YTHDF1 (1:1000, 17479-1-AP, Proteintech), rabbit anti-YTHDF2 (1:1000, 24744-1-AP, Proteintech), rabbit anti-YTHDF3 (1:1000, 25537-1-AP, Proteintech), rabbit anti-IGF2BP1 (1:1000, 22803-1-AP, Proteintech), rabbit anti-IGF2BP2 (1:1000, 11601-1-AP, Proteintech), rabbit anti-IGF2BP3 (1:1000, 14642-1-AP, Proteintech), rabbit anti-flag (1:1000, 80010-1-RR, Proteintech), mouse anti-Myc (1:1000, 60003-2-Ig, Proteintech), rabbit anti-MATR3 (1:1000, 12202-2-AP, Proteintech), mouse anti-JNK (1:1000, 66210-1-Ig, Proteintech), rabbit anti-phosphorylated JNK (1:1000, ab131499, Abcam), rabbit anti-p38 (1:1000, ab170099, Abcam), rabbit anti-phosphorylated p38 (1:1000, ab4822, Abcam), rabbit anti-ERK (1:1000, ab17942, Abcam), rabbit anti-phosphorylated ERK (1:1000, ab214036, Abcam). After incubation with specific secondary antibodies (1:10000, Kangwei, China), membranes were developed using the ECL kit (Pierce, USA).

Co-IP (Co- immunoprecipitation) assay and MS (tandem mass spectrometry) analysis

Macrophages were lysed and centrifuged to collect the supernatant. One tenth of the supernatant was retained for the input immunoblot, while the rest was incubated with anti-Mettl3/Mettl14/Matr3 antibodies or IgG at 4 °C overnight, followed by further incubation with 10 μl protein A/G-agarose beads (Cell Signaling Technology, USA) for another 4 h. The bound proteins were subjected to washing three times for a total of 30 min and then eluted by boiling for 5 min in the loading buffer. Immunocomplexes were analyzed by SDS-PAGE electrophoresis and then incubated with anti-Mettl3/Mettl14/Matr3 antibodies.

Native PGAE

Macrophages in 10 cm dish were transfected with pCMV3-N-FLAG-Mettl3 plasmid and/or pCMV3-N-Myc-Matr3 for 24h. Then the cells were treated with oxLDL (40 μg/ml) or not for 24h. Next, the cells were

collected and lysed for Co-immunoprecipitation assay as above method. The eluted proteins were separated on an 8% non-denaturing polyacrylamide gel in the Tris-Glycine native PAGE running buffer (pH = 8.8; without SDS) and the transferred membrane used for Western blotting as above.

Me-RIP (methylated RNA-binding protein immunoprecipitation) and Seq

Me-RIP was conducted using the Magna RIP kit (Millipore, USA). In brief, the cells were harvested after washing twice with 1× PBS and then lysed with RIP lysis buffer. The supernatant was incubated with antibodies against m6A overnight at 4 °C. Then, 50 μl A/G magnetic beads were added to the supernatant and incubated for 6 h. After immobilizing the magnetic bead bound complexes with a magnetic separator (Millipore USA), supernatants were used to extract RNA with PCA (phenol: chloroform: isoamyl alcohol) reagent at a ratio of 125:24:1 (Aladdin, USA). Then, the immunoprecipitation (IP) (m6A-seq) library was constructed, and sequenced by Novogene (Beijing, China).

RNA-binding protein immunoprecipitation (RIP)

RIP was performed as previously described using the Magna RIP kit (Millipore, USA)[23]. Briefly, the cells were harvested after washing twice with 1× PBS and then lysed with RIP lysis buffer. The supernatant was incubated with antibodies against Matr3 (ab281947, Abcam), m6A (ab286164, Abcam), YTHDF1 (17479-1-AP, ProteinTech), YTHDF2 (24744-1-AP, ProteinTech), YTHDF3 (25537-1-AP, ProteinTech), or IgG overnight at 4 °C. Then, 50 μl A/G magnetic beads were added to the supernatant and incubated for 6 h. After immobilizing the magnetic bead bound complexes with a magnetic separator (Millipore USA), supernatants were used to extract RNA with PCA (phenol: chloroform: isoamyl alcohol) reagent at a ratio of 125:24:1 (Aladdin, USA). A cDNA synthesis kit (ABI USA) was used to synthesize the first cDNA strand from mRNA. Finally, qRT-PCR was performed using the following primers: PGC1-α, 5'-ACTACAGACACCGCACACACC-3', and 5'-CCTTTCGTGCTCATAGGCTTC-3'; Map3k11, 5'-CCTTGTTCCCGGACTCAGAC-3', and 5'-GGCACCCATGTCTTTGGTCT-3'; Mapk14, 5'-GCTGTGAATGAAGACTGTGAGC-3', and 5'-AGGAGCCCTGTACCACCTAG-3'; TNFAIP1, 5'-CACACACACCCAAAGGAGGA-3', and 5'-GCTTGTCCGCTCGTGTTTTT-3'; IFNAR1, 5'-AAAAATACAGTTCCCAAACTAGCCA-3', and 5'-TCATACAAAGTCCTGCTGTAGTTCT-3'; and ARG1, 5'-GGACCCTGGGGAACACTACA-3', and 5'-GTGTTTCTTCCATCACCTTGCC-3'.

Analysis of protein-protein interaction

The proteins interacted with Mettl3 or Mettl14 were analyzed with Biogrid database (https://thebiogrid.org/).

Immunofluorescence

Macrophages were seeded in 35-mm glass bottom dishes, fixed and permeabilized at 4°C for 30 min. After incubation with anti-Mettl3 antibody (67733-1-Ig, Proteintech), and anti-Matr3 antibody (ab240123, Abcam) antibody at 4°C overnight, the cells were washed with PBS twice and stained with goat-anti-rabbit FITC-labelled IgG or goat-anti-mouse Alexa Fluor® 594-labelled IgG (abcam, USA) at 4°C for 2 h, followed

by DAPI staining. The cells were viewed using a Zeiss Confocal Microscope Imaging System (Carl Zeiss, Germany).

Fluorescence in situ hybridization (FISH)

Macrophages were first fixed in 4% formaldehyde solution, and then incubated with 0.5% Triton X-100. RNA was stained using SYTO^{TM} RNAselect^{TM} Green (S32703) at 37 °C with cells in the dark for 30 min. Then, the cells were incubated with anti Matr3 antibody (ab240123, Abcam) antibody at 4°C overnight, and incubated with Goat Anti-Rabbit IgG H&L (Alexa Fluor® 594) (abcam, USA) at 4°C for 2 h, followed by DAPI staining. The cells were then photographed using a Zeiss Confocal Microscope Imaging System (Carl Zeiss, Germany).

Enzyme-linked immunosorbent assay (ELISA) assays

Macrophages in 12 well-plates were transfected with pCMV3-N-Myc-Matr3 or pCMV3-N-Myc empty plasmid (EV) for 24h. Then the cells were treated with oxLDL (40 μg/ml) or not for 24h. Post-culture media was then collected and subjected to ELISA assays specific for IL-6 and TNF-α using the Human IL-6 ELISA Kit (ab178013, Abcam) and the Human TNF alpha ELISA Kit (ab181421, Abcam), respectively.

Single-cell RNA sequencing (scRNA-seq) analysis

The R package Monocle was used for pseudotime trajectory analysis: T cell single-cell level expression profiling was extracted from single-cell RNA sequencing datasets(GSE154692) in mouse atherosclerotic aortas, and monocle CellDataSet(CDS) object was constructed with expression matrix and reported metadata. After normalizing prepared CDS object, differential genes test was performed among different cell types using differentialGenenTest function. Then top 3000 differentially expressing genes (DEGs) ranked by q-value were applied as candidate features for re-clustering and ordering cells. To find out most representative markers for each state of T cell evolution, DEG test was again performed according to pseudo-time state, and top 50 varied DEGs were clustered for pseudotime-ordered heatmap with plot_pseudotime_heatmap function.

mRNA stability assays

Macrophages were transfected with pCMV3-N-Myc-Matr3 or pCMV3-N-Myc empty plasmid (EV) for 24h, then were incubated with actinomycin D (5 μg/ml) for 0 h, 6 h or 12 h followed by RNA extraction. The half-life of MAP3K11 and MAPK14 mRNAs were analyzed by qRT-PCR.

Biochemistry assay for m6A methyltransferase activity in vitro

In vitro methyltransferase activity assay was performed in a standard 50 μL of reaction mixture containing the following components: 0.15 nmol total mRNA, recombinant Matr3 protein or recombinant Mettl14 protein, 0.8 mM d3-SAM, 80 mM KCl, 1.5 mM $MgCl_2$, 0.2 U μL-1 RNasin, 10 mM DTT, 4% glycerol, and 15 mM HEPES (pH 7.9). The reaction was incubated at 16 °C for 12 h. The resultant RNA was

recovered by phenol/chloroform (low pH) extraction followed by ethanol precipitation, and digested by nuclease P1 and alkaline phosphatase for QQQ LC-MS/MS analysis. The nucleosides were quantified by using the nucleoside to base ion mass transitions of 285 to 153 (d3-m6A) and 284 to 152 (G). G served as an internal control to calculate the amount of RNA probe in each reaction mixture.

Animal experiments and atherosclerosis analysis

$APOE^{-/-}$ mice were purchased from Nanjing Model Animal Research Center and housed in the Laboratory Animals Center of the first affiliated hospital Zhejiang university school of medicine, with controlled temperature and humidity. All experimental procedures were approved by the Animal Care Ethics Committee of the Zhejiang University. $APOE^{-/-}$ mice were fed with a high fat high cholesterol diet (Western Diet) for 12 weeks to induce atherosclerosis. 16 $ApoE^{-/-}$ mice were randomly divided into two groups (8 mice/group): normal $ApoE^{-/-}$ mice fed with normal diet group (Control), and $APOE^{-/-}$ mice fed with a high fat high cholesterol diet. To explore the effect of Matr3 on atherosclerosis development in *vivo*, 16 $ApoE^{-/-}$ mice were randomly selected, and 8 of them were injected with the control Lentivirus (NC) (1.0×10^8 particles) via tail vein as the control group, while the remaining $ApoE^{-/-}$ mice were injected with Matr3-overexpressing Lentivirus (1.0×10^8 particles) which was obtained from GenePharma (Shanghai, China). Two weeks after the lentiviral injection, the mice were fed with Western Diet for 12 weeks to induce atherosclerosis. 12 weeks later, the mice were anesthetized with sodium pentobarbital (50 mg/kg, i.p.; BHD, Canada). After exposing the abdominal cavity and rapid opening of the right atrium, 5 ml of saline was slowly injected into the left ventricle along the apex of the heart to wash the blood. Next, 4% polyformaldehyde was slowly injected to fix the vascular tissue morphology for 30 min. Thereafter, the aorta and perivascular adipose tissue were removed under a stereomicroscope. The pulmonary arteriovenous malformation was excised, and then the artery together with the heart was removed, followed by placement in 4% paraformaldehyde at room temperature overnight. The aortas were dissected, and whole aortas were opened longitudinally from the aortic arch to the iliac bifurcation, mounted en face, and stained for lipids with Oil Red O and hematoxylin-eosin (Jiancheng, China). Image analysis was performed by a trained observer blinded to the genotype of the mice. Representative images were obtained, and lesion areas were quantified with Image J.

Statistical analysis

Data are presented as the mean ± standard deviation (SD). The differences between two groups were compared by t-test. The differences among multiply groups were compared using ANOVA analysis. A P value of< 0.05 was considered statistically significant and all experiments were repeated at least three times.

Results

1. oxLDL stimulation decreases m6A modification level in macrophages.

To investigate the role of m6A modification on macrophages mediated-inflammatory responses during atherosclerosis development, the total m6A modification levels of macrophage treated with oxLDL treatment were measured. As shown in Fig. 1A, oxLDL stimulation significantly decreased m6A modification level in macrophages in a dose-dependent manner. Furthermore, we found that oxLDL stimulation significantly increases the methyltransferases Mettl3 and Mettl14 expressions in macrophages (Fig. 1B), whereas oxLDL stimulation does not evidently affect the expressions of m6A "Reader" proteins, including Ythdf/2/3 and Igf2bp1/2/3. Unexpected, oxLDL stimulation decreased the interaction between Mettl3 and Mettl14 (Supplemental Fig. 1A). Subsequently, transcriptome-wide m6A methylome profiled by methylated RNA immunoprecipitation sequencing (MeRIP-seq) was performed. As shown in Fig. 1D, m6A peak is mainly enriched between genebody and the down-stream 2000 bp of genebody, and mostly distributes on coding sequence (CDS) and stop codon regions (Supplemental Fig. 1B) in macrophages stimulated with oxLDL or not. Motif analysis reveals both groups enriched GGACU as the highest score motif (Supplemental Fig. 1C), suggesting that MeRIP-seq possess high quality. As shown in Fig. 1E and supplemental Fig. 1D, we identified 1438 RNAs with gain of methylation and 2146 RNAs with loss of methylation. Kyoto Encyclopedia of Genes and Genomes (KEGG) analysis indicates that genes with differential m6A modification were enriched in the metabolic pathways and pro-inflammatory signaling pathways, including mitogen-activated protein kinase (MAPK) (Fig. 1F). Overall, these results indicate that although oxLDL stimulation increases methyltransferases Mettl3 and Mettl14 expressions in macrophages, the total m6A modification level in macrophages decreases under oxLDL stimulation.

Matrin-3 (Matr3) promotes the formation of Mettl3-Mettl14 complex formation.

To explore the underlying mechanism of oxLDL stimulation reducing the interaction of Mettl3 and Mettl14 in macrophages, we searched the binding proteins of Mettl3 or Mettl14 *in Biogrid database* (Supplemental Fig. 2A and 2B) and found there are 91 proteins in the both binding spectrum of Mettl3 and Mettl14 (Fig. 2A). Then, we evaluated the proteins with the high score hits, and found there are 11 RNA binding domains (RRM)-containing proteins, including EIF4B, EWSR1, FUS, MATR3 and etc. Given that mutations in Matr3 have been reported to alter protein-protein interactions and impede mRNA nuclear export[24], we suspect whether Matr3 has a potential role in the formation of Mettl3-Mettl14 complex. Co-IP analysis showed that endogenous Matr3 indeed had weak binding on endogenous Mettl14 in macrophages (Fig. 2B), but had strong binding on endogenous Mettl3 (Fig. 2C). Furthermore, Co-IP analysis also confirmed the interaction between exogenous Myc-labelled Matr3 and Flag-labelled Mettl3 (Fig. 2D), and Immunofluorescence analysis showed that Mettl3 was strictly co-localized with Matr3 in the nucleus (Fig. 2E). Moreover, we found that oxLDL stimulation significantly decreased the interaction of Mettl3 and Matr3 (Fig. 2F). In addition, ectopic over-expression of Matr3 significantly increased the formation of Mettl3-Mettl14 complex (Fig. 2G), and knockdown of Matr3 reduced (Fig. 2H). Finally, native-PAGE analysis also showed oxLDL stimulation significantly reduces the formation of Mettl3-Mettl14 complex, whereas overexpression of Matr3 alleviates the inhibitor effects of oxLDL on the formation of Mettl3-Mettl14 complex (Fig. 2I). Overall, these results indicate that Matr3 promotes the formation of Mettl3-Mettl14 complex formation.

Matr3 is involved in promoting mRNA m6A modifications, which depends on the Mettl3-Mettl14 complex.

Since Matr3 participates in the formation of Mettl3-Mettl14 complex, we suspected whether Matr3 acts as a partner of m6A catalytic subunit. To verify our hypothesis, we purified full-length Matr3, Mettl3, Mettl14 proteins (Fig. 3A, and Supplemental Fig. 2C) and performed *in vitro* total mRNA modification experiments. As shown in Fig. 3B and Supplemental Fig. 2D, LC-MS/MS analysis indicated that overexpression of Matr3 does not significantly affect the m^6A level in polyadenylated RNA, whereas overexpression of Mettl14 evidently increased the m^6A level. Next, we detected whether Matr3 affected the m6A modification on peroxisome proliferator-activated receptor gamma coactivator 1-alpha (PGC-1α) mRNA, which has been reported to occur m6A modification by Mettl3 to promote mitochondrial dysfunction and oxLDL-induced inflammation in monocytes[25] (Supplemental Fig. 2E). As shown in Fig. 3C, overexpression of Matr3 significantly increased the m6A modifications on PGC-1α mRNA. However, Matr3 did not directly bind to PGC-1α mRNA (Fig. 3D). Moreover, immunofluorescence analysis showed that Matr3 merely has partially co-location with RNA in nucleus (Fig. 3E). Finally, we found that knockdown of Mettl3 nearly cancelled the up-regulatory effect on the m6A modification on PGC-1α mRNA of Matr3 (Fig. 3C, 3F). Overall, these results indicate that Matr3 is involved in promoting mRNA m6A modification, which depends on the Mettl3-Mettl14 complex.

Matr3 inhibits oxLDL-induced the activation of MAPK pathway via m6A-mediated mRNA decay.

Given that MAPK pathway acts important roles in oxLDL-induced macrophage activation and inflammatory responses[26, 27], and MAPK signaling-related genes were enriched in our MeRIP-seq results (Fig. 1F and Fig. 4A), we then explored the effects of Matr3 on oxLDL-induced the activation of MAPK pathway in macrophages. As shown in Fig. 4B, overexpression of Matr3 significantly increased the m6A modification on MAPK pathway-related genes, such as Map2k7 and Map3k11, inflammatory-related genes, type 1 IFN receptor chain 1 (INFAR1), and Arginase-1 (Arg-1). Besides, overexpression of Matr3 significantly increased the binding of Ythdf2/3 on Map2k7 and Map3k11 (Fig. 4C). Considering that Ythdf2 and Ythdf3 are reported to regulate pre-mRNA splicing and RNA decay[28, 29], we further investigated whether Matr3 affected the stability of Map2k7 and Map3k11 mRNAs, and found that overexpression of Matr3 significantly promoted Map3k11 and Mapk14 mRNAs degradation (Fig. 4D and 4E). Moreover, we found that overexpression of Matr3 significantly decreased oxLDL-induced the up-regulated phosphorylation expressions of P38 and JNK (Fig. 4F). In addition, overexpression of Matr3 also significantly inhibited oxLDL-induced the up-regulated expressions of inflammatory factors, IL-6 and TNFα in macrophages (Fig. 4G and 4H). Overall, these results indicate that Matr3 suppresses oxLDL-induced inflammatory responses in macrophages through promoting MAPK pathway-related gene decay by Ythdf2/3.

oxLDL stimulation decreases Matr3 protein expression in macrophages in an m6A-YTHDF2-dependent manner.

Next, to investigate whether oxLDL stimulation affects Matr3 expression in macrophages, we re-analyzed the published single-cell RNA sequencing (scRNA-seq) data of atherosclerotic plaque derived macrophages (GSE154692). As shown in Fig. 5A and Supplemental Fig. 3A, during macrophage differentiation and macrophage polarization, Matr3 expression decreased in pro-inflammatory macrophages. Furthermore, RT-PCR, immunofluorescence, and Western blotting analysis verified that oxLDL stimulation significantly reduces MATR3 mRNA and protein expressions in macrophages (Fig. 5B, 5C and 5D). Subsequently, to explore the regulatory mechanism of Matr3 expression in macrophages under oxLDL stimulation, we detected the m6A modification levels on Matr3 and found oxLDL did not influence the m6A modification level of Matr3 mRNA (Fig. 5E), suggesting that oxLDL stimulation affecting Matr3 protein expression may be depends on post-transcriptional regulation. Furthermore, sequencing mapping analysis showed that new m6A modification sites appeared on the CDS region of Matr3 mRNA under oxLDL stimulation, indicating m6A sites on Matr3 mRNA shift (Supplemental Fig. 3B). Moreover, RIP and mRNA stability analysis showed that oxLDL stimulation evidently promoted Ythdf2 binding on Matr3 mRNA in macrophages (Fig. 5F) and promoted Matr3 mRNA decay (Fig. 5G). Overall, these results indicate that oxLDL stimulation decreases Matr3 protein expression in macrophages in an m6A-YTHDF2-dependent manner.

Matr3 alleviates atherosclerosis development in vivo.

To further investigate the role of Matr3 on atherosclerosis development *in vivo*, atherosclerosis mice model was established using ApoE-/- mice fed with western diet (WD). As shown in Fig. 6A, immunofluorescent staining showed that Matr3 expression in the CD68-positive macrophages in the atherosclerotic plaque area of APOE-/- mice was significantly lower, compared to the normal control group. Besides, m6A modification level in the CD68-positive macrophages in the atherosclerotic plaque area was also significantly decreased, compared to the normal control group (Fig. 6B). Next, Matr3 overexpression in APOE-/- mice was established by injected with lentiviruses via the tail vein, and then fed with western diet to induce atherosclerosis. En face aorta analysis showed that the lesion area was significantly smaller in the LV-Matr3 group, compared to control LV-NC group (Fig. 6C), and HE analysis also confirmed (Fig. 6D). Finally, we further examined the m6A level and Matr3 expression level in peripheral blood mononuclear cells (PBMCs) from patients with coronary artery disease (CAD) or health volunteers (N). As shown in Fig. 6E and 6F, consistent to our hypothesis, m6A modification level and Matr3 protein expression levels were significantly decreased in the CAD group, compared to control. Collectively, these results indicate that Matr3 alleviates atherosclerosis development *in vivo*, and Matr3 expression is decreased in the peripheral blood mononuclear cells from patients with CAD.

Discussion

Atherosclerosis is characterized as the chronic inflammation of the arterial wall, and eventually leads to acute cardiovascular events[30]. As atherosclerosis cases rise year by year globally, illuminating the underlying mechanism of atherosclerosis is getting more and more attention. Besides smoking, hypercholesterolemia, hypertension, hyperglycemia, and genetic factors function important roles in

atherosclerosis[11–14], global trends in Atherosclerosis research is in the epigenetics field nowadays[31]. Recent study reports a marked downregulation of m6A in rRNA through analyzing carotid atherosclerotic lesion samples representing early and advanced stages of atherosclerosis compared to non-atherosclerotic arteries from healthy controls[21]. In this study, we explored the roles of m^6A methylation on macrophages-mediated inflammatory response during atherosclerosis, and found that oxLDL stimulation increases methyltransferases Mettl3 and Mettl14 expressions in macrophages, whereas the total m6A modification level in macrophages decreases under oxLDL stimulation. We firstly identify Matr3 as protective factor, which inhibits activation of pro-inflammatory signaling, mitogen-activated protein kinase (MAPK) by m6A-mediated mRNA decay via regulating the formation of Mettl3-Mettl14 complex in macrophages.

Matr3, as an RNA-binding nuclear protein, plays vital roles in regulating chromosomal and genomic integrity, RNA-binding mediated post-transcriptional mRNA regulation, and nuclear lamina association to maintain nuclear framework[32, 33]. Recently, mutations in Matr3 have been to be involved in the pathopoiesis of amyotrophic lateral sclerosis by altering protein-protein interactions and impeding mRNA nuclear export[24]. In this study, we find that Matr3 expression is decreased in the oxLDL-stimulated macrophages, and the peripheral blood mononuclear cells from patients with CAD, and overexpression of Matr3 significantly inhibits oxLDL-induced inflammatory responses in macrophages, and alleviates atherosclerosis development. In mechanism, Matr3 inhibits oxLDL-induced activation of pro-inflammatory signaling, mitogen-activated protein kinase (MAPK) by m6A-mediated mRNA decay via regulating the formation of Mettl3-Mettl14 complex in macrophages. Previous study identified approximately 50 Matr3 interacting proteins in NSC-34 cells, and most of these proteins are within the TRanscription and Export (TREX) protein complex that regulates mRNA nuclear export[24]. Whether Matr3 also affects the nuclear export of inflammation-related genes in macrophages during atherosclerosis development needs further investigation. In addition, Matr3 expression in neural stem cells has been suggested to maintain the undifferentiated state, albeit limited to morphological observations[34]. Through re-analysis of the scRNA-seq data of atherosclerotic plaque derived macrophages, we find that during macrophage differentiation and macrophage polarization, Matr3 expression decreased in pro-inflammatory macrophages. Whether Matr3 is involved in the macrophage differentiation and macrophage polarization during during atherosclerosis development needs to be further investigated in the following studies.

Mettl3-Mettl14 methyltransferase complex has been studied widely for its role in generating m6A formation within an RRACH sequence context in RNA[35]. Recent study has reported that the Mettl3-Mettl14 methyltransferase complex methylates its target RNAs not only sequence but also secondary structure dependent. RNA secondary structure dependence in Mettl3-Mettl14 mRNA methylation is modulated by the N-terminal domain of Mettl3[36]. In this study, we find that Matr3 has weak binding on Mettl14 in macrophages, but has strong binding on Mettl3. Whether Matr3 interacting with Mettl3 enhances the methyltransferase activity of Mettl3-Mettl14 complex, and whether Matr3 affects the function of the N-terminal domain of Mettl3 need to be further investigated.

In conclusion, out study explores the roles of m^6A methylation on macrophages-mediated inflammatory response during atherosclerosis. We for the first time identifies Matr3 to function a suppressive role on oxLDL-mediated macrophage inflammatory responses through inhibiting activation of MAPK signaling by m6A-mediated mRNA decay via regulating the formation of Mettl3-Mettl14 complex, resulting in alleviating atherosclerosis development. Although the relationships between m6A modification and atherosclerosis are still unclear and need more attention in the future, our study suggests Matr3 may be a potential target for atherosclerosis treatment.

Declarations

Declaration of competing interest

All authors declare no conflict of interest.

Acknowledgements

We thank Liangrong Zheng for suggestions for the study.

Availability of data and materials

The dataset(s) supporting the conclusions of this article are included within the article and its additional files.

Authors' contributions

ZW S, S W, J Z and WT Z conceived and designed the experiments. ZW S, WJ C, Z W, S W performed the experiments and analyzed the data. J Z and WT Z wrote the manuscript. All authors read and approved the manuscript.

Funding

This study was supported by National Natural Science Foundation of China (No.82000316 and No. 81873484) and Science and Technology Planning Project of Guangzhou (No. 202102020119).

References

1. Torres N, Guevara-Cruz M, Velazquez-Villegas LA, Tovar AR. Nutrition and Atherosclerosis. Arch Med Res. 2015;46:408–26.
2. Rognoni A, Cavallino C, Veia A, Bacchini S, Rosso R, Facchini M, Secco GG, Lupi A, Nardi F, Rametta F, Bongo AS. Pathophysiology of Atherosclerotic Plaque Development. Cardiovasc Hematol Agents Med Chem. 2015;13:10–3.
3. Moore KJ, Sheedy FJ, Fisher EA. Macrophages in atherosclerosis: a dynamic balance. Nat Rev Immunol. 2013;13:709–21.

4. Sakakura K, Nakano M, Otsuka F, Ladich E, Kolodgie FD, Virmani R. Pathophysiology of atherosclerosis plaque progression. Heart Lung Circ. 2013;22:399–411.
5. Pirillo A, Norata GD, Catapano AL. LOX-1, OxLDL, and atherosclerosis. Mediators Inflamm. 2013;2013:152786.
6. Couto NF, Rezende L, Fernandes-Braga W, Alves AP, Agero U, Alvarez-Leite J, Damasceno N, Castro-Gomes T, Andrade LO. OxLDL alterations in endothelial cell membrane dynamics leads to changes in vesicle trafficking and increases cell susceptibility to injury. Biochim Biophys Acta Biomembr. 2020;1862:183139.
7. Ito F. Polyphenols can Potentially Prevent Atherosclerosis and Cardiovascular Disease by Modulating Macrophage Cholesterol Metabolism. Curr Mol Pharmacol. 2021;14:175–90.
8. Menegaut L, Jalil A, Thomas C, Masson D. Macrophage fatty acid metabolism and atherosclerosis: The rise of PUFAs. Atherosclerosis. 2019;291:52–61.
9. Cheng AY, Leiter LA. Implications of recent clinical trials for the National Cholesterol Education Program Adult Treatment Panel III guidelines. Curr Opin Cardiol. 2006;21:400–4.
10. Wang C, Wang F, Cao Q, Li Z, Huang L, Chen S. Effect and safety of combination lipid-lowering therapies based on statin treatment versus statin monotherapies on patients with high risk of cardiovascular events. Aging Med (Milton). 2018;1:176–84.
11. Siasos G, Tsigkou V, Kokkou E, Oikonomou E, Vavuranakis M, Vlachopoulos C, Verveniotis A, Limperi M, Genimata V, Papavassiliou AG, Stefanadis C, Tousoulis D. Smoking and atherosclerosis: mechanisms of disease and new therapeutic approaches. Curr Med Chem. 2014;21:3936–48.
12. Wang HH, Garruti G, Liu M, Portincasa P, Wang DQ. Cholesterol and Lipoprotein Metabolism and Atherosclerosis: Recent Advances In reverse Cholesterol Transport. Ann Hepatol. 2017;16:s27–42.
13. Soliman GA. Dietary Fiber, Atherosclerosis, and Cardiovascular Disease. Nutrients. 2019;11.
14. Fontanella RA, Scisciola L, Rizzo MR, Surina S, Sardu C, Marfella R, Paolisso G, Barbieri M. Adiponectin Related Vascular and Cardiac Benefits in Obesity: Is There a Role for an Epigenetically Regulated Mechanism? Front Cardiovasc Med. 2021;8:768026.
15. Herman AB, Occean JR, Sen P. Epigenetic dysregulation in cardiovascular aging and disease. J Cardiovasc Aging. 2021;1.
16. Zhang N, Zuo Y, Peng Y, Zuo L. Function of N6-Methyladenosine Modification in Tumors. J Oncol. 2021;2021:6461552.
17. Zhang C, Liu J, Guo H, Hong D, Ji J, Zhang Q, Guan Q, Ren Q. m6A RNA methylation regulators were associated with the malignancy and prognosis of ovarian cancer. Bioengineered. 2021;12:3159–76.
18. Wang Y, Li L, Li J, Zhao B, Huang G, Li X, Xie Z, Zhou Z. The Emerging Role of m6A Modification in Regulating the Immune System and Autoimmune Diseases. Front Cell Dev Biol. 2021;9:755691.
19. Zhao Y, Shi Y, Shen H, Xie W. m(6)A-binding proteins: the emerging crucial performers in epigenetics. J Hematol Oncol. 2020;13:35.

20. Li Y, Bedi RK, Moroz-Omori EV, Caflisch A. Structural and Dynamic Insights into Redundant Function of YTHDF Proteins. J Chem Inf Model. 2020;60:5932–5.
21. Quiles-Jimenez A, Gregersen I, Mittelstedt LDSM, Abbas A, Kong XY, Alseth I, Holm S, Dahl TB, Skagen K, Skjelland M, Aukrust P, Bjoras M, Halvorsen B. N6-methyladenosine in RNA of atherosclerotic plaques: An epitranscriptomic signature of human carotid atherosclerosis. Biochem Biophys Res Commun. 2020;533:631–7.
22. Chien CS, Li JY, Chien Y, Wang ML, Yarmishyn AA, Tsai PH, Juan CC, Nguyen P, Cheng HM, Huo TI, Chiou SH, Chien S. METTL3-dependent N(6)-methyladenosine RNA modification mediates the atherogenic inflammatory cascades in vascular endothelium. Proc Natl Acad Sci U S A. 2021;118.
23. Zhao W, Wang Z, Sun Z, He Y, Jian D, Hu X, Zhang W, Zheng L. RNA helicase DDX5 participates in oxLDL-induced macrophage scavenger receptor 1 expression by suppressing mRNA degradation. Exp Cell Res. 2018;366:114–20.
24. Boehringer A, Garcia-Mansfield K, Singh G, Bakkar N, Pirrotte P, Bowser R. ALS Associated Mutations in Matrin 3 Alter Protein-Protein Interactions and Impede mRNA Nuclear Export. Sci Rep. 2017;7:14529.
25. Zhang X, Li X, Jia H, An G, Ni J. The m(6)A methyltransferase METTL3 modifies PGC-1alpha mRNA promoting mitochondrial dysfunction and oxLDL-induced inflammation in monocytes. J Biol Chem. 2021;297:101058.
26. Du H, Zhang H, Yang R, Qiao L, Shao H, Zhang X. Small interfering RNA-induced silencing lncRNA PVT1 inhibits atherosclerosis via inactivating the MAPK/NF-kappaB pathway. Aging. 2021;13:24449–63.
27. Zhou J, Ma W, Wang X, Liu H, Miao Y, Wang J, Du P, Chen Y, Zhang Y, Liu Z. Matrine Suppresses Reactive Oxygen Species (ROS)-Mediated MKKs/p38-Induced Inflammation in Oxidized Low-Density Lipoprotein (ox-LDL)-Stimulated Macrophages. Med Sci Monit. 2019;25:4130–6.
28. Yen YP, Chen JA. The m(6)A epitranscriptome on neural development and degeneration. J Biomed Sci. 2021;28:40.
29. Shi H, Wei J, He C. Where, When, and How: Context-Dependent Functions of RNA Methylation Writers, Readers, and Erasers. Mol Cell. 2019;74:640–50.
30. Hansson GK, Hermansson A. The immune system in atherosclerosis. Nat Immunol. 2011;12:204–12.
31. Doehring A, Geisslinger G, Lotsch J. Epigenetics in pain and analgesia: an imminent research field. Eur J Pain. 2011;15:11–6.
32. Malik AM, Miguez RA, Li X, Ho YS, Feldman EL, Barmada SJ. Matrin 3-dependent neurotoxicity is modified by nucleic acid binding and nucleocytoplasmic localization. Elife. 2018;7.
33. Zeitz MJ, Malyavantham KS, Seifert B, Berezney R. Matrin 3: chromosomal distribution and protein interactions. J Cell Biochem. 2009;108:125–33.
34. Niimori-Kita K, Tamamaki N, Koizumi D, Niimori D. Matrin-3 is essential for fibroblast growth factor 2-dependent maintenance of neural stem cells. Sci Rep. 2018;8:13412.

35. Schibler U, Kelley DE, Perry RP. Comparison of methylated sequences in messenger RNA and heterogeneous nuclear RNA from mouse L cells. J Mol Biol. 1977;115:695–714.
36. Meiser N, Mench N, Hengesbach M. RNA secondary structure dependence in METTL3-METTL14 mRNA methylation is modulated by the N-terminal domain of METTL3. Biol Chem. 2020;402:89–98.

Figures

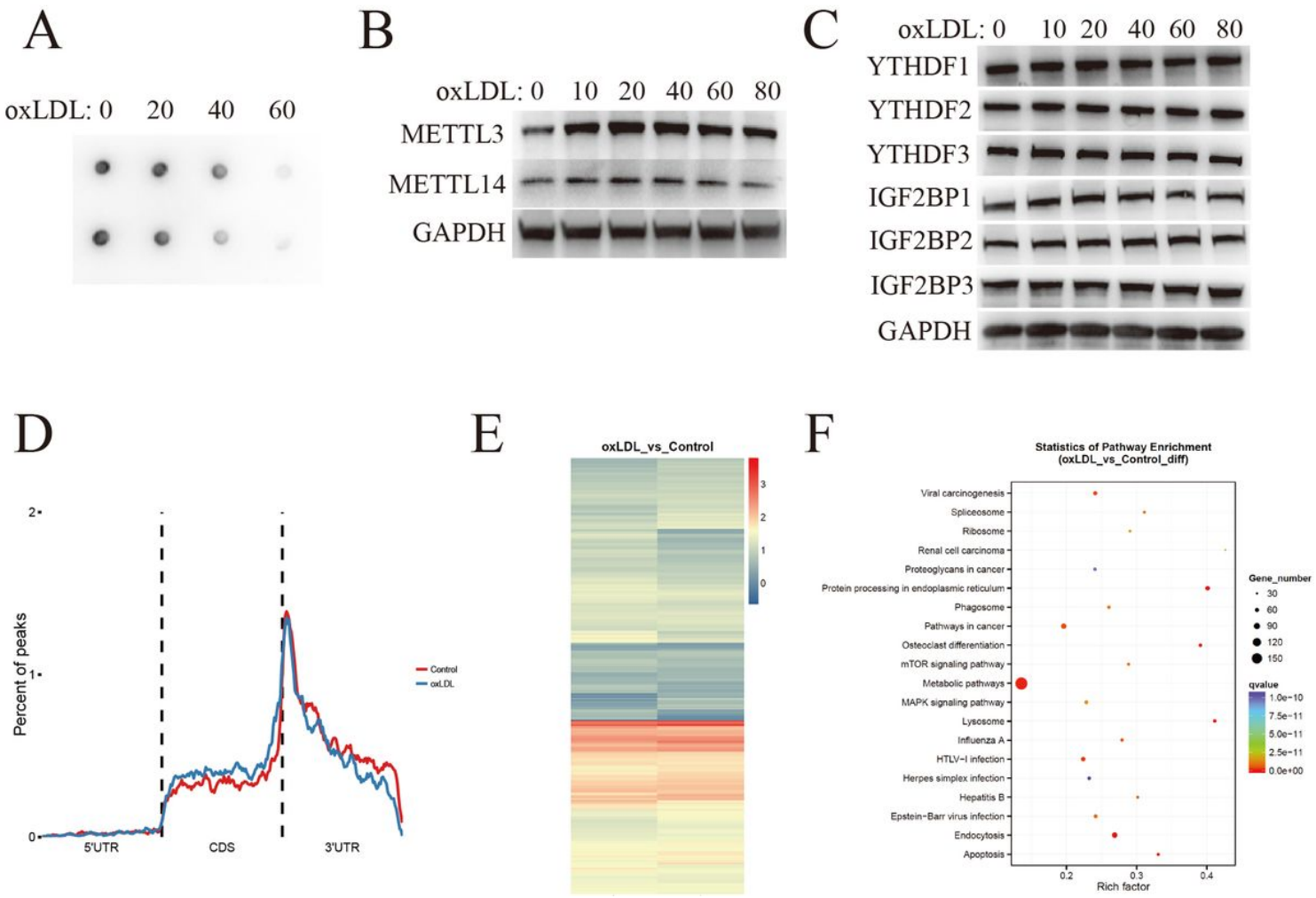

Figure 1

oxLDL stimulation decreases m6A modification level in macrophages. A: Detection of m6A modification levels of total RNA from oxLDL-treated macrophages by dot blot; B and C: Western blotting analysis of the indicated proteins in macrophages treatment with various concentrations of oxLDL for 24h (GAPDH as an endogenous control); D: The distributions of m6A peak on the mRNA regions in the control and oxLDL-treated groups; E: Heatmap analysis of differentially expressed genes between control and oxLDL-treated groups; F: KEGG pathway analysis of differentially expressed genes between control and oxLDL-treated groups.

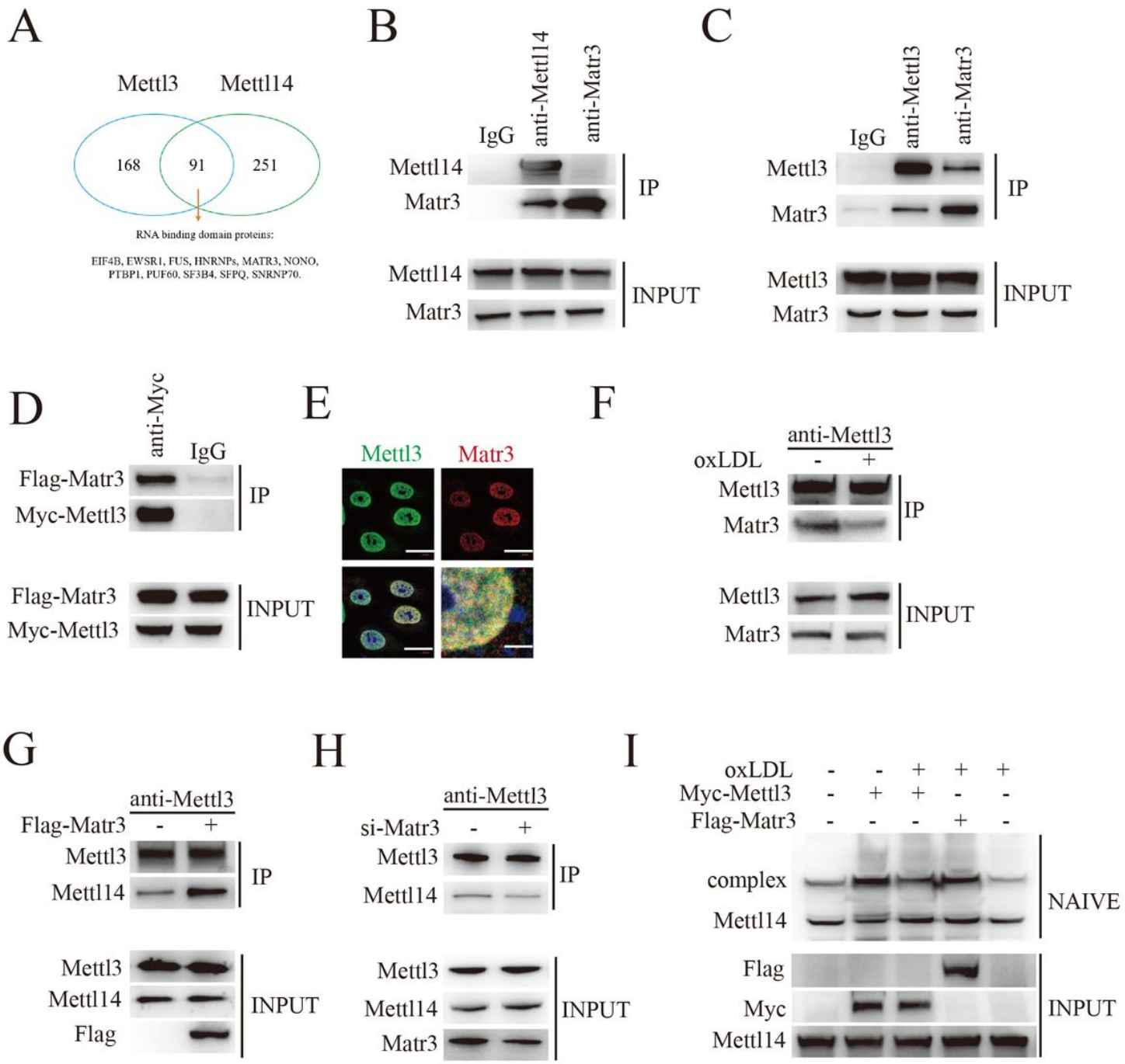

Figure 2

Matrin-3 (Matr3) promotes the formation of Mettl3-Mettl14 complex formation.

A: Venn diagram of Metll3 and Mettl14 interacting proteins; B: co-IP analysis of the interaction of Matr3 and Mettl14 in macrophages; C: co-IP analysis of the interaction of Matr3 and Mettl3 in macrophages; D: co-IP analysis of the interaction of Myc-Matr3 and Flag-Mettl3 in 293T cells transfected with pCMV3-N-MYC-Mettl3 plasmid and pCMV3-N-FLAG-Matr3 plasmid for 24h; E: Fluorescence analysis of the co-localization of Mettl3 and Matr3 in macrophages (Nucleus, blue); F: co-IP analysis of the interaction of Matr3 and Mettl3 in macrophages treated with oxLDL (40 μg/ml) or not for 24h with anti-Mettl3

antibodies; G: co-IP analysis of the interaction of Mettl3 and Mettl14 in macrophages transfected with pCMV3-N-FLAG-Matr3 with anti-Mettl3 antibodies; H: co-IP analysis of the interaction of Mettl3 and Mettl14 in macrophages transfected with si-Matr3 with anti-Mettl3 antibodies; I: Macrophages were transfected with pCMV3-N-MYC-Mettl3 plasmid and/or pCMV3-N-FLAG-Matr3 plasmid for 24h, and then treated with oxLDL (40 μg/ml) or not for 24h. co-IP analysis of the interaction of Mettl3 and Mettl14 using anti-Mettl14 antibody with native-gels.

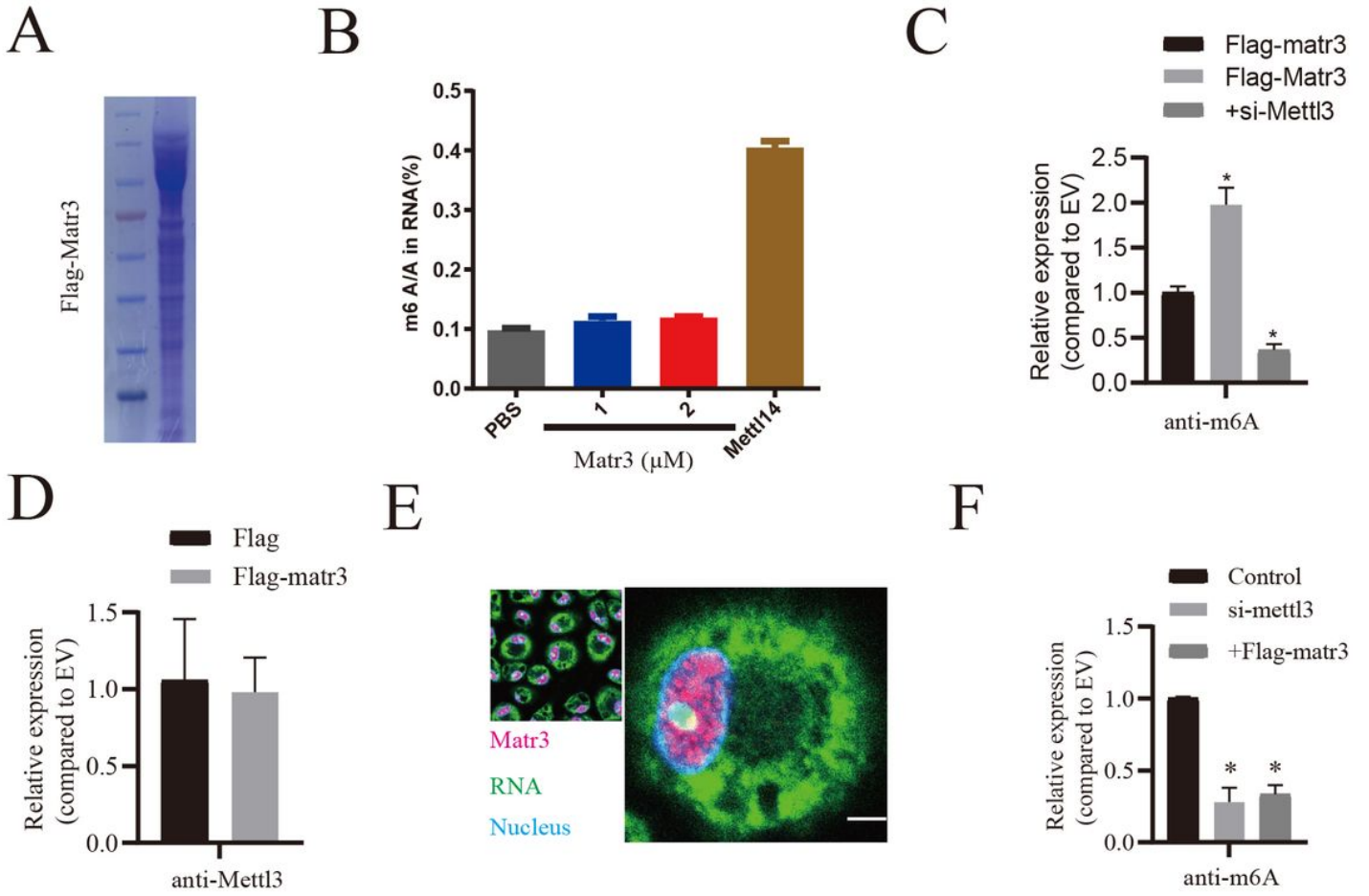

Figure 3

Matr3 is involved in promoting mRNA m6A modifications, which dependents on the Mettl3-Mettl14 complex.

A: Coomassie blue staining of purified Flag-tagged Matr3 recombinant proteins; B: LC-MS/MS analysis of the m6A/A percent in total mRNA in macrophages transfected with pCMV3-N-FLAG-Mettl14 plasmid or pCMV3-N-FLAG-Matr3 plasmid; C: RIP analysis of the m6A modification level on the PGC-1α mRNA in macrophages transfected with pCMV3-N-FLAG-Matr3 plasmid or pCMV3-N empty vector by anti-m6A antibodies; D: RIP analysis of the interaction of Matr3 and PGC-1α mRNA in macrophages transfected with pCMV3-N-FLAG-Matr3 plasmid or pCMV3-N empty vector by anti-FLAG antibodies; E: FISH analysis of the co-localization of Matr3 and PGC-1α mRNA in macrophages (Nucleus, blue); F: RIP analysis of the m6A modification level on the PGC-1α mRNA in macrophages transfected with pCMV3-N empty vector,

pCMV3-N-FLAG-Matr3 plasmid and pCMV3-N-FLAG-Matr3 plasmid+si-Mettl3 by anti-m6A antibodies. $^{*}P < 0.05$. The data represent three independent experiments.

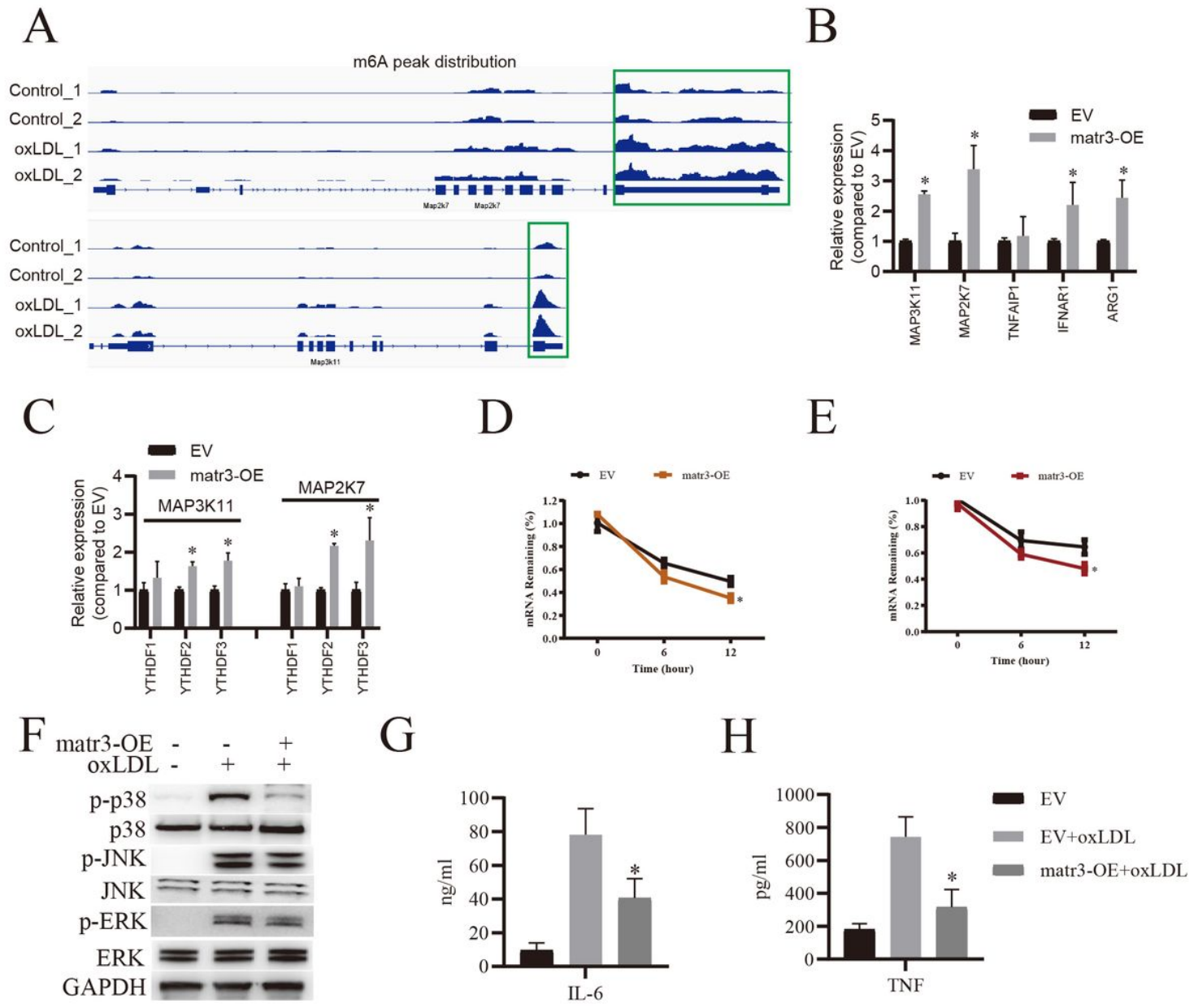

Figure 4

Matr3 inhibits oxLDL-induced MAPK pathway activation dependent on m6A-mediated mRNA decay.

A: MeRIP-seq mapping analysis of the distributions of m6A peak on Map2k7 and Map3k11 genes; B: RIP analysis of the m6A modification levels on Map3k11, Map2k7, Tnfaip1, Ifnar1 and Arg1 mRNAs in macrophages transfected with pCMV3-N empty vector (EV) or pCMV3-N-Myc-Matr3 plasmid by anti-m6A antibodies; C: RIP analysis of the interactions of YTHDF1/2/3 and Map3k11/Map2k7 mRNA in macrophages transfected with pCMV3-N empty vector (EV) or pCMV3-N-FLAG-Matr3 plasmid by anti-YTHDF1/2/3 antibodies; D: qRT-PCR analysis of the stability of Map3k11 mRNA in macrophages transfected with pCMV3-N empty vector (EV) or pCMV3-N-FLAG-Matr3 plasmid; E: qRT-PCR analysis of

the stability of Map2k7 mRNA in macrophages transfected with pCMV3-N empty vector (EV) or pCMV3-N-FLAG-Matr3 plasmid; F: Western blotting analysis of the indicated proteins in macrophages transfected with pCMV3-N empty vector (EV) or pCMV3-N-FLAG-Matr3 plasmid for 24h, and then treated with oxLDL (40 μg/ml) for 24h; G and H: ELISA analysis of the IL-6 or TNA-α secretions in macrophages transfected with pCMV3-N empty vector (EV) or pCMV3-N-FLAG-Matr3 plasmid for 24h, and then treatment with oxLDL (40 μg/ml) for 24h. $^{*}P < 0.05$. The data represent three independent experiments.

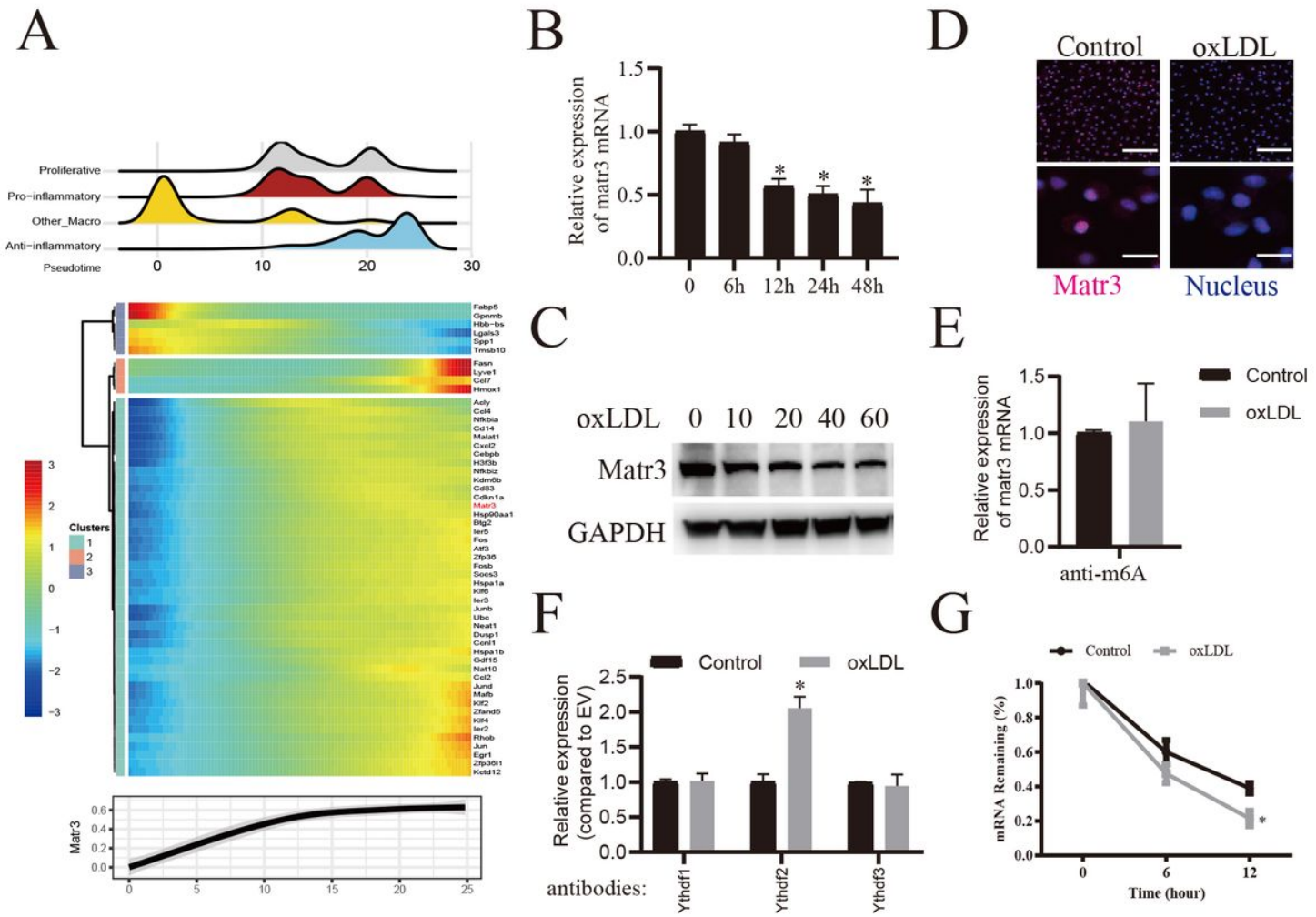

Figure 5

oxLDL stimulation decreases Matr3 protein expression in macrophages in an m6A-YTHDF2-dependent manner.

A: scRNA-seq analysis of Matr3 expression during the phenotype transformation of macrophages (upper: macrophages subtypes; middle: pseudo-time analysis; bottom: Matr3 expression change); B: qRT-PCR analysis of Matr3 mRNA expression in macrophages treated with oxLDL (40 μg/ml) for different hours; C: Western blotting analysis of Matr3 protein expression in macrophages treated with oxLDL for 24h; D: Fluorescence analysis of the distribution of Matr3 in macrophages treated with oxLDL (40 μg/ml) or not for 24h (Nucleus, blue); E: RIP analysis of the m6A modification levels on Matr3 mRNA in macrophages

treated with oxLDL (40 μg/ml) for 24h; F: RIP analysis of the interaction of Ythdf1/2/3 protein and Matr3 mRNA in macrophages treated with oxLDL (40 μg/ml) for 24h; G: qRT-PCR analysis of the stability of Matr3 mRNA in macrophages treated with oxLDL (40 μg/ml) or not for 24h. $^{*}P < 0.05$. The data represent three independent experiments.

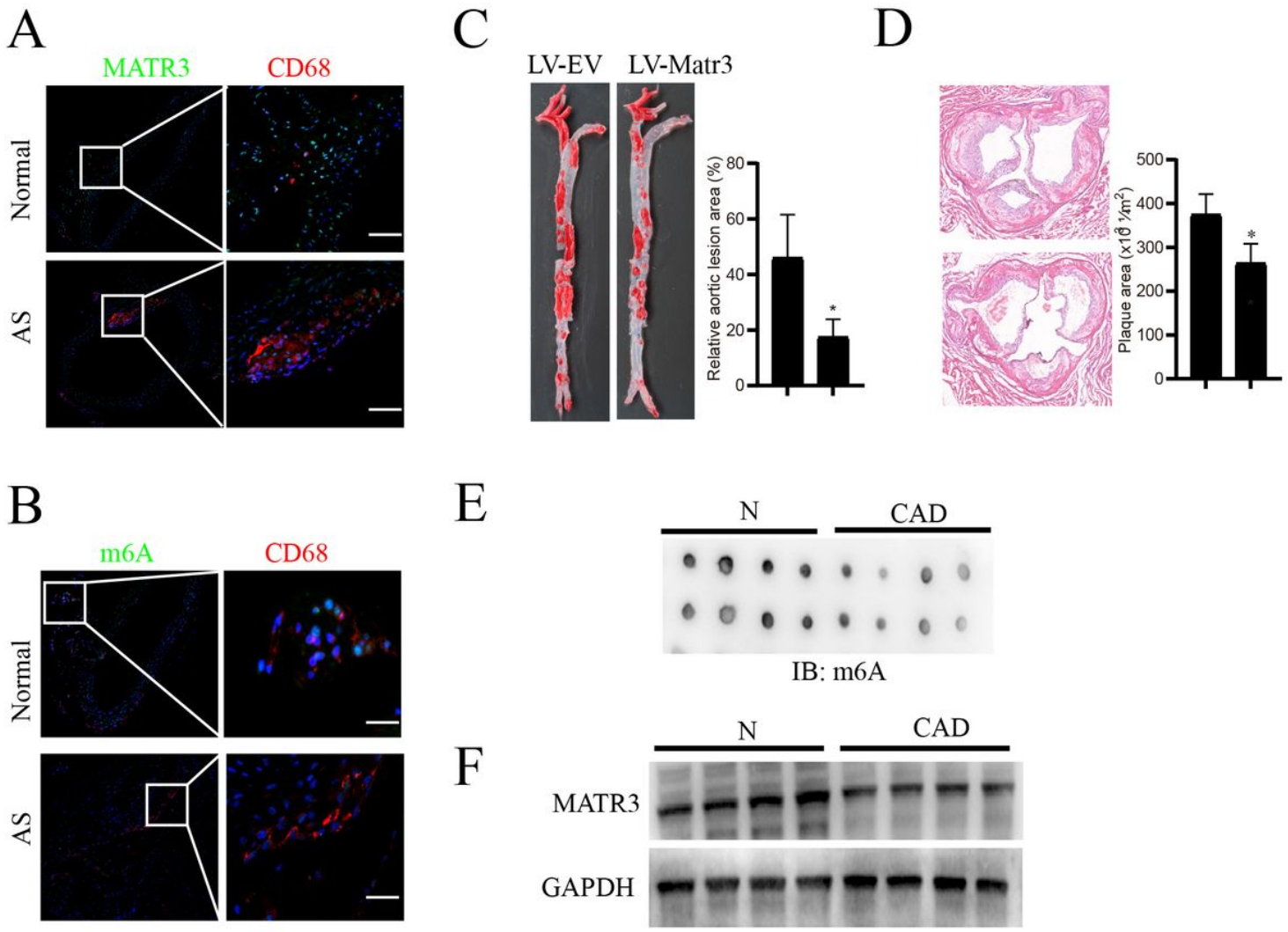

Figure 6

Matr3 alleviates atherosclerosis development *in vivo.*

A: Immunofluorescence analysis of Matr3 (green) and CD68 (red) expression in the normal aortic regions of normal mice (Control) or atherosclerotic plaque regions of AS model mice, respectively; B: Immunofluorescence analysis of m6A (green) and CD68 (red) expression in the normal aortic regions of normal mice (Control) or atherosclerotic plaque regions of AS model mice, respectively; C: Representative images and quantification of the aorta en face lesion stained with oil red O in the indicated group (n=8); D: Representative images and quantification of the aortic necrotic core area stained with HE in the aortic root (n=8); E: dot blot analysis of m6A modification levels of total RNA in PBMCs isolated from health

volunteers or patients with CAD; F: Western blot analysis of Matr3 protein expression in PBMCs isolated from health volunteers or patients with CAD.

Supplementary Files

This is a list of supplementary files associated with this preprint. Click to download.

- supplementarymaterials.doc